Optimization Using a Shared and Distributed X-in-the-Loop Testing Environment

Viktor Schreiber, Valentin Ivanov, *Senior Member, IEEE*

***Abstract*—X-in-the-loop (XIL) technologies have been receiving increased attention in modern automotive development processes. In particular, collaborative experiments using XIL tools have efficient applications in the design of multi-actuated, electric, and automated vehicles. The presented paper introduces results of such a collaborative study with XIL, which focused on the feasibility of coordinated real-time (RT) simulations for the control of vehicle dynamics systems. The outcomes are based on extensive co-simulation tests performed with remote connections among different geographical locations. The performed study allowed formulating requirements for further shared and distributed XIL-experiments for functional validation of automotive control systems.**

***Index Terms*—X-in-the-loop, co-simulation, vehicle models, automotive control, remote tests, optimization.**

I. Introduction

IMPROVING functionality is one of key issues in model-based system engineering. Usually, the development of novel systems is based on heuristic experience or empirical data. However, insufficient knowledge about the technical system can lead to a poor design outcome. To address this aspect, the paper introduces an approach for optimization in a multi-domain X-in-the-Loop testing environment according to Fig. 1, [1], and [2]. In particular, *simultaneous perturbation stochastic approximation* (SPSA) was chosen as typical representation of recursive, robust optimization and was adapted to the X-in-the-Loop method. It does not require any explicit knowledge about the system to create an analytical model for optimization. Instead, empirical data from the X-in-the-Loop environment is used to optimize the problem with a generic loss function. The synergy of these two methods combines their advantages so that testing and developing a system can be done simultaneously to save effort and development time.

II. Optimization method

Spall et al. introduces in SPSA a user-defined perturbation ε that simultaneously varies the parameter θ to estimate the gradient of the loss function. Each gradient estimation is differentiated by the corresponding loss function $L_\mathrm{k}(\theta \pm \xi\varepsilon)$, and the finite difference interval ξ is formed. [3], [4]

$$\theta_{\mathrm{k+1}} = \theta_\mathrm{k} \pm \psi_\mathrm{k}\, g_\mathrm{k}(\theta) \tag{1a}$$

$$g_\mathrm{k}(\theta) = \frac{L_\mathrm{k}^{(+)} - L_\mathrm{k}^{(-)}}{2\xi_\mathrm{k}\varepsilon_\mathrm{k}} \tag{1b}$$

$$L_\mathrm{k}^{(\pm)} = L_\mathrm{k}(\theta_\mathrm{k} \pm \xi_\mathrm{k}\varepsilon_\mathrm{k}) \tag{1c}$$

V. Schreiber and V. Ivanov are with Technische Universität Ilmenau, Germany.

A. State space representation

Robbins-Monro, Kiefer-Wolfowitz and Spall derived their original consideration using scalar sequences and a one-dimensional parameter θ. However, engineering systems are usually multidimensional problems. Therefore, the scalar problem is transferred to a state space, which applies in the same way to one-dimensional systems.

Let there exist a linear state space with the input vector $\underline{\boldsymbol{x}} \in \mathbb{R}^{n\times 1}$ and the output vector $\underline{\boldsymbol{y}} \in \mathbb{R}^{m\times 1}$. The input and output vectors are linearly combined over the parameter space $\underline{\hat{\boldsymbol{\theta}}} \in \mathbb{R}^{m\times n}$, so that Eq. 2 holds. At each time k there exists a sample of all states.

$$\underbrace{\begin{bmatrix} y_1 \\ \vdots \\ y_m \end{bmatrix}_\mathrm{k}}_{\underline{\boldsymbol{y}}_\mathrm{k}} = \underbrace{\begin{bmatrix} \hat{\theta}_{11} & \cdots & \hat{\theta}_{1n} \\ \vdots & \ddots & \vdots \\ \hat{\theta}_{m1} & \cdots & \hat{\theta}_{mn} \end{bmatrix}}_{\underline{\hat{\boldsymbol{\theta}}}} \underbrace{\begin{bmatrix} x_1 \\ \vdots \\ x_n \end{bmatrix}_\mathrm{k}}_{\underline{\boldsymbol{x}}_\mathrm{k}} \tag{2}$$

Because of the singularity of $\underline{\hat{\boldsymbol{\theta}}}$ the method is not applicable for state space representations. Therefore we reduce the state space representation to a system of equations with single outputs.

$$y_{\mathrm{m,k}} = \underbrace{\begin{bmatrix} \hat{\theta}_{m1} & \cdots & \hat{\theta}_{mn} \end{bmatrix}}_{\underline{\hat{\boldsymbol{\theta}}}_\mathrm{m}} \underbrace{\begin{bmatrix} x_1 \\ \vdots \\ x_n \end{bmatrix}_\mathrm{k}}_{\underline{\boldsymbol{x}}_\mathrm{k}} \tag{3}$$

The corresponding recursive rule of the SPSA optimization is described in Eq. 4 and Eq. 5.

$$\underline{\boldsymbol{\theta}}_{\mathrm{k+1}}^T = \underline{\boldsymbol{\theta}}_\mathrm{k}^T \pm \underline{\hat{\boldsymbol{g}}}_\mathrm{k}^T \underline{\boldsymbol{\psi}}_\mathrm{k} \tag{4}$$

$$\underline{\hat{\boldsymbol{g}}}_\mathrm{k}^T = \frac{1}{2}\left[\underline{\boldsymbol{L}}_\mathrm{k}^{(+)} - \underline{\boldsymbol{L}}_\mathrm{k}^{(-)}\right]\left[\underline{\boldsymbol{\xi}}_\mathrm{k}\underline{\boldsymbol{\varepsilon}}_\mathrm{k}^T\right]^{-1} \tag{5}$$

B. Tuning

To achieve convergence specific criteria for the sequences of ξ and ψ, the user-specified distribution of ε and the statistical relationship between ε and the measurements $Y(\theta)$ is required [4]. Although Kiefer/Wolfowitz and Spall give some hints for implementation, the methods are formulated generically [5], [4]. This gap is closed under the framework of XIL, and the following problems will be correspondingly discussed:

(i) The sequences ξ and ψ have to be chosen, so that the convergence criteria is satisfied.

(ii) An end condition for seeking θ to an optimal solution $\hat{\theta}$ has to be carried out. The convergence of sequence ξ needs to be taken into account for the end condition.

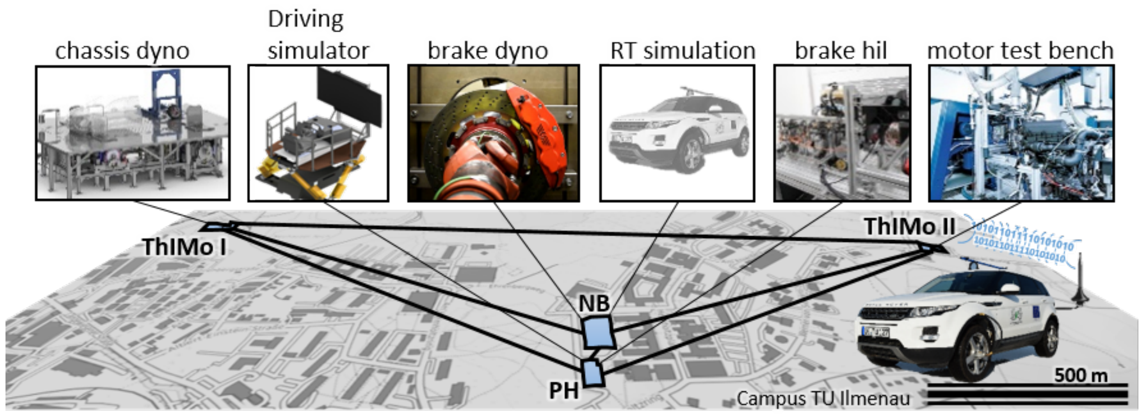

Fig. 1. Local distributed X-in-the-Loop testing environment built in campus of Technische Universität Ilmenau

(iii) Since the gradient $g(\theta)$ might have noise, a suitable distribution for ε must be chosen.
(iv) Depending on the optimization problem, a suitable loss function $L(\theta)$ must be selected.
(v) For simultaneous running of optimization and testing, the methods have to be real-time capable.

$$\sum_{\mathrm{k}=0}^{\infty} \psi_{\mathrm{k}} = \infty \tag{6}$$

$$\sum_{\mathrm{k}=0}^{\infty} \psi_{\mathrm{k}} \xi_{\mathrm{k}} < \infty \tag{7}$$

$$\sum_{\mathrm{k}=0}^{\infty} \psi_{\mathrm{k}}^2 \xi_{\mathrm{k}}^{-2} < \infty \tag{8}$$

For satisfaction the boundary conditions the sequencen ξ and ψ was chosen according to Eq. 9 und Eq. 10, where γ musst be smaller than α. ξ and ψ must converge to zero not too fast and not too slow.

$$\psi_{\mathrm{k}} = \hat{\psi}(C+k)^{-\alpha} \tag{9}$$

$$\xi_{\mathrm{k}} = \hat{\xi}(D+k)^{-\gamma} \tag{10}$$

The sequence ε is supposed to be independent of the measurement and symmetrically distributed around zero. The Bernoulli distribution and Monte Carlo distribution (zero-one distribution) can satisfy these requirements [3], [6]. Uniform distributions or normal distributions are not suitable, since these do not have an inverse moment for all ε.

$$\varepsilon_{\mathrm{k}} = \begin{cases} +1 & P(\varepsilon \in 1) = 0.5 \\ -1 & P(\varepsilon \in -1) = 1 - P(\varepsilon \in 1) \end{cases} \tag{11}$$

The parameters for SPSA optimization of ABS were tuned according to Tab. I.

TABLE I
PARAMETER SETUP FOR SPSA

parameter	value/Eq.
α	0.9
γ	0.7
C	1
D	1
ψ_1	1^{-6}
$\hat{\theta}$	10^9
K	5000
$\hat{\psi}$	$\psi_1(C+K)^{\alpha}$
$\hat{\xi}$	$\hat{\theta}(D+1)^{\gamma}$

C. Improvement of robustness and constraints

Robustness refers to a fail-safe system or method that responses resistant against failure, disturbances, and uncertainties. A robust fail-safe system is not aware of any possible disturbance. It is sufficient if the most likely failure scenarios are considered in the designing process. Therefore, for a robust system, its operation in a wide range of possible frequencies should be usually studied. Looking at the different forms of excitation, four basic types emerge in Fig. 2: (a) Dirac impulse, (b) step, (c) (harmonic) sine sweep, and (d) (randomized) noise. While the frequency range of the Dirac pulse determines by the duration in time domain, the step response excites only a low-frequency range. In contrast, the sine sweep and noise excite almost to the entire frequency range. However, the realization of the waveforms proves to be challenging. Since the system must be settled during excitation with sine sweep the frequency must be increasing slowly. Furthermore, it is not feasible to optimize problems for low frequencies using the sine sweep signal. Consequently, the sine sweep requires experimental design with long periods, the Dirac pulse cannot be realized for some automotive systems (e.g. ABS) and the excited frequency range of the step function is not sufficient. Although the power density of noise is very low in the frequency domain, the authors recommend to use randomization for improving the robustness of optimization problems. It excites simultaneous the entire bandwidth including low frequencies, since the duration of experiments is limited.

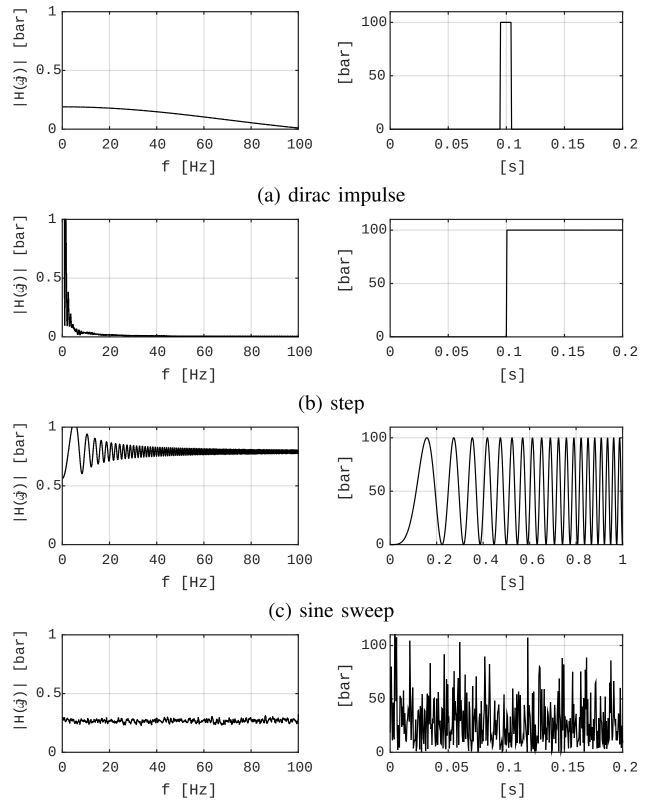

(a) dirac impulse

(b) step

(c) sine sweep

(d) noise

Fig. 2. Benchmark of excitation waveforms in time domain and frequency domain

As an feasible implementation of noise, two experimental setups will be introduced in a nutshell. This will be considered in next sections as applied to the anti-lock braking control with decoupled electro-hydraulic brake system Considering typical tasks of the ABS control, the reference slip is firstly randomized for the controller that enables seeking for its stability. Second, the friction coefficient of the road tire contact must be distributed randomly. The combination of these measures is discussed with reference to Fig. 3.

D. Convergence and termination criterion for SPSA

Compared to FDSA, SPSA does not require at least the same number of iterations as the number of samples. The SPSA method can work with only two representative samples to be able fully functional [7]. However, decreasing as the number of samples or iteration steps reduce the accuracy significant. But it saves computational costs.

To reduce the effort the recursion must be abort ahead of schedule. Therefore an assessment to measure the quality of parameter optimization must be utilized. Assuming that no confidential system model can be obtained for the loss function, the stochastic convergence criterion according to Eq. 12 can be used. For values below 1 the solution converges, for values equal 1 no assessment can be made and for values larger than 1 the solution diverges.

$$Q = \frac{\sum |y_\mathrm{k} - \boldsymbol{\theta}_\mathrm{k} \boldsymbol{x}_\mathrm{k}|}{|\sum y_\mathrm{k}|} \tag{12}$$

If the quality Q becomes smaller then a certain threshold S, the solution have reaches the equilibrium. For instance, 5% is a reasonable value for S. This means the iteration can be abort, when the boundary condition $Q < S$ is fullfilled.

E. Real-time capability

Regardless of the lack of an implementation method, the SPSA method offers great potential for real-time systems, since the number of required iterations can be kept within reasonable effort. However, SPSA is not designed for real-time, therefore real-time capability will be investigated briefly.

It can be clearly stated that the number of iterations K depending on the amount of samples and system dynamics represented by the highest frequency ω.

$$K \propto \omega^{\beta} \tag{13}$$

Based on an observation period, the solution of the optimization algorithm must converge within this time slot. The duration of the observation period T, the number of iterations K and the sampling rate T_s obtain the real-time capability according to Eq. 14.

$$T_s < \frac{T}{K} \tag{14}$$

III. Optimization of brake system related problems

A brake blending case study was chosen to demonstrate the principle of optimization using a shared and distributed XIL testing environment. Since advanced brake systems allow a high dynamic brake pressure modulation, a continuous ABS controller shown in Eq. 15 - 20 is selected in this study.

This use case introduce a wide range of phenomena and requires a robust design under consideration of several uncertainties related to the friction brake behaviour, road conditions and miscellaneous non-linear system responses. At that the actuation dynamics is also constraint by the decoupled character of the braking system.

A. Continuous ABS controller

The control philosophy of conventional ABS are rule-based algorithms, which are typically divided into the three phases of pressure build-up, pressure hold, and pressure release [8]. However, the complexity of rule-based ABS increased for advanced brake systems as components of integrated vehicle dynamics control. Even when the algorithm is tuned optimal, the wheel can be purposefully locked for a short period to find the optimal wheel slip with maximum coefficient of adhesion according to the characteristics from Fig. 4. Alternatively, the decoupled electro-hydraulic brake systems enable closed-loop control, since the wheel brake pressure can be determined. In [9], Savitski et. al present an architecture for electrohydraulic braking systems and investigate the performance of various continuous ABS algorithms such as the PI controller, the sliding mode PI, or the integral sliding mode. Based on these methods and for the purpose of the PID controller, the demanded brake pressure p^* is determined from base brake pressure p^*_{BB}, which is modulated with the ABS brake

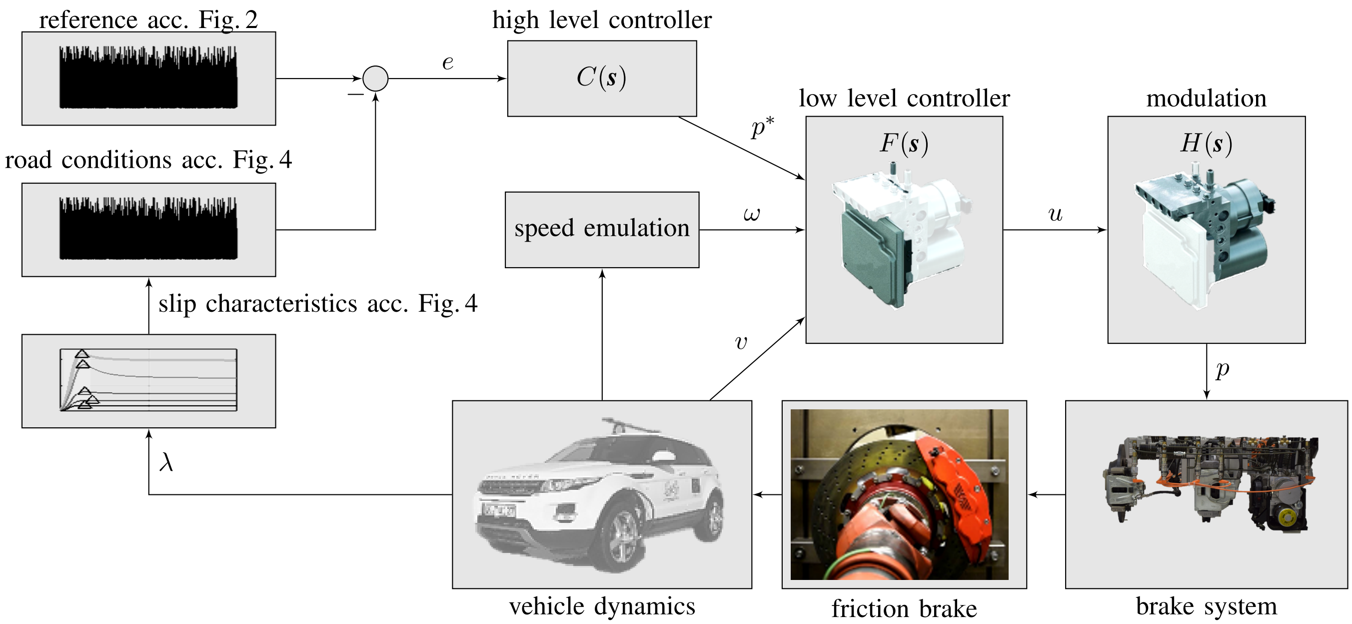

Fig. 3. Proposed experimental setup for robust optimization of continuous ABS

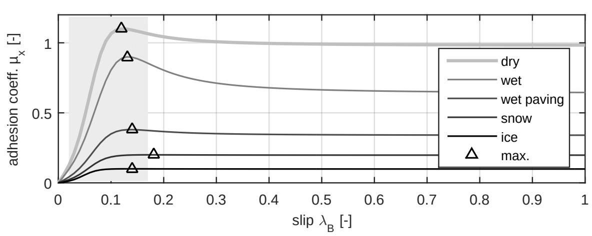

Fig. 4. Characteristic slip curve

pressure p^*_{ABS} in accordance with Eq. 18. The total demand of braking torque M^* derives from wheel brake torque M^*_{WB} and the torque of the in-wheel motor M^*_{IWM}. Whereby the wheel brake torque derives from a specific brake rated value B^* including the friction coefficient, the friction radius, number of friction pairs, piston area, and others.

$$M^* = M^*_{WB} + M^*_{IWM} \tag{15}$$

$$M^*_{WB} = B^* p^* \tag{16}$$

$$p^* = p^*_{BB} - p^*_{ABS} \tag{17}$$

$$p^*_{ABS} = K_P e + K_I \int e \, \partial t + K_D \frac{\partial e}{\partial t} \tag{18}$$

$$e = \lambda^*_B - \lambda_B \tag{19}$$

$$\lambda_B = \frac{v - \omega \times r_z}{v} \tag{20}$$

The performance of the ABS controller depends on the parameters K_P, K_I, K_D, and on the estimate of the reference slip λ^*_B, at which the maximum tire-road friction coefficient can be utilized. Usually, these parameters are determined empirically. Alternatively, Savitski et. al have also shown in [9] an experimentally validated method for seeking the reference slip λ^*_B in real-time. For this reason, the authors focus on the optimization of the parameters K_P, K_I and K_D in this study.

B. Experimental setup

The experimental setup is based on hardware-in-the-loop (HIL) test methods for the development of electro-hydraulic brake systems. As Fig. 3 illustrates, in this procedure a low level controller (embedded ECU) and mechatronic components (EHB) are integrated in a simulation. In automotive testing, this procedure is also referred to bus simulation, since communication between ECUs takes place via bus communication. In the distributed XIL environment the authors are using UDP communication over VPN as a gateway for exchanging information corresponding to [2]. This demands hard real-time requirements for the simulation in a way that a native behavior of the vehicle can be kept, and the ECU does not notice any difference between a virtual and physical vehicle. Compared to road tests, experiments using the HIL methodology can be performed with high reproducibility. In addition, further physical phenomena can be taken into account by a brake dynamometer according to the test-rig-in-the-loop methodology [2]. For this purpose, the RT simulation demands brake pressure from the brake HIL. The measured brake pressure from the HIL is forwarded to a brake dynamometer, which sends feedback as the braking torque into the RT simulation, where the vehicles motion is emulated. The tire-road contact dynamics is also covered by the simulation. A more detailed description of this XIL testing environment can be found in [2].

It should be noted that the reference slip is set as the white noise in next tests to improve the robustness by optimization using XIL. The friction coefficient between road and tire is distributed randomly. This enables an excitation of a wide frequency bandwidth.

C. Loss function and optimization problem

A proper definition of the loss function is crucial for optimization problems. For control applications the control error e must be minimized. Therefore we define the loss function as the error to the power of two: $L = e^2$. When the gradient $\frac{\partial L}{\partial \theta}$ from the control error reaches zero, the minimum is located.

Brake blending for the considered vehicle configuration is a combined optimization problem with trade-off between the operation of the brake system and the in-wheel motor. Therefore, we reduce the problem to one common function, as shown in Eq. 21. Here, every unique loss function L_i is normalized and weighted by the weighting factors w_i.

$$\underline{\boldsymbol{L}} = \frac{1}{\sum w_i} \sum w_i L_\text{i} \tag{21}$$

For the brake system the loss function L_1 is defined according Eq. 22, where the noisy brake pressure p^*_{ABS} was chosen as controller reference y_1 on purpose.

$$\begin{aligned} \underline{\boldsymbol{L}}_1 &= (\underline{\boldsymbol{y}}_1 - \underline{\boldsymbol{\theta}}\, \underline{\boldsymbol{x}}_1)^2 && \text{(22a)} \\ \underline{\boldsymbol{y}}_1 &= p^*_{ABS} && \text{(22b)} \\ \underline{\boldsymbol{x}}_1 &= \begin{bmatrix} e & \int e \partial t & \frac{\partial e}{\partial t} \end{bmatrix}^T && \text{(22c)} \\ \underline{\boldsymbol{\theta}}_1 &= \begin{bmatrix} K_P & K_I & K_D \end{bmatrix} && \text{(22d)} \end{aligned}$$

The loss function of the in-wheel controller is defined by Eq. 23, where the noisy reference torque M^*_{IWM} was chosen on purpose.

$$\begin{aligned} \underline{\boldsymbol{L}}_2 &= (\underline{\boldsymbol{y}}_2 - \underline{\boldsymbol{\theta}}\, \underline{\boldsymbol{x}}_2)^2 && \text{(23a)} \\ \underline{\boldsymbol{y}}_2 &= M^*_{IWM} && \text{(23b)} \\ \underline{\boldsymbol{x}}_2 &= \begin{bmatrix} e & \int e \partial t & \frac{\partial e}{\partial t} \end{bmatrix}^T && \text{(23c)} \\ \underline{\boldsymbol{\theta}}_2 &= \begin{bmatrix} C_P & C_I & C_D \end{bmatrix} && \text{(23d)} \end{aligned}$$

Assuming that the braking torque and the motor should engage likewise, they are weighted by 0.5. Considering that the loss functions have different measures, they have to be normalized in addition. Given that the brake torque arrives from the specific brake value B^* and the brake pressure, the loss function for the in-wheel motor is normalized by $(\frac{1}{B^*})^2$. It should be noted that the weighting factors are individually tailored and must be adapted to the specific requirements for a particular vehicle. The derived weighting factors $w_1 = 0.5$ and $w_2 = 0.5(\frac{1}{B^*})^2$ are merely examples. The higher the weighting factor the more the loss function is taken into account for the optimization.

IV. Experimental results

Shared and distributed testing domains like Model-in-the-Loop, Hardware-in-the-Loop, Test-Rig-in-the-Loop and X-in-the-Loop are intended to compare the optimization performance. For proof of concept, a use case for brake systems will be demonstrated according to Fig. 1.

A. Parameter identification

As indicated in Fig. 5, the optimization process is steady. The parameters were identified already after approximately 1000 iterations on the front axle. On the rear axle, significantly more iteration steps are needed to identify the integral parameter K_I. This result is typical because of vehicle dynamics. The parameter K_D was not depicted in Fig. 5 because

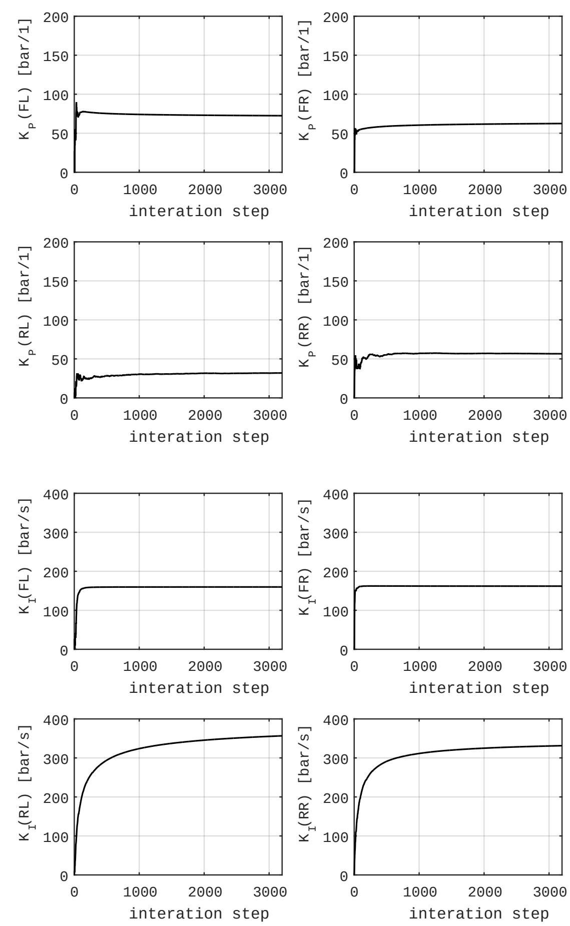

Fig. 5. History of SPSA optimization of ABS using XIL

the optimization method did not identified this parameter as considerable.

During braking the vehicle initiates to pitch due to the major wheel load redistribution to the front axle. Consequently, the rear axle is less loaded and the corresponding wheels tend to lock. This phenomena can be observed in Fig. 6 for the wheel speeds. Fig. 6 also indicates that the brake pressure is randomly modulated as proposed for optimization process. To improve the convergence on the rear axle, the SPSA must be adjust to it. However, faster convergence could adversely affect the robustness of the optimization method.

B. Test run after SPSA optimization using xil

In this work, different XIL methodologies derived from [2] were used for benchmark the optimization of ABS for electric vehicles. Specifically a parameter optimization using the model-in-the-loop (RT simulation), hardware-in-the-loop

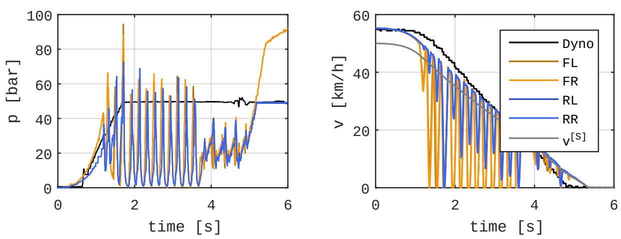

Fig. 6. Test run during SPSA optimization using XIL

(brake HIL), and test-rig-in-the-loop (brake dyno TRIL) were carried out. The fusion of all methods is referred as X-in-the-loop. It is remarkable, that the MIL and TRIL methods delivers the highest values for K_P. The reason for this lies in the fidelity of the model. In this regard the brake system was considered as reduced order model (ROM). Complex physical phenomena such as dynamics of the friction coefficient of brakes, transfer behavior of the brake system, and the dynamics of the low level controller are not taken into account properly. Hence, using the parameter from MIL or TRIL optimization can cause instabilities of the high level controller on a real ECU. In general the parameter K_P is bigger on the

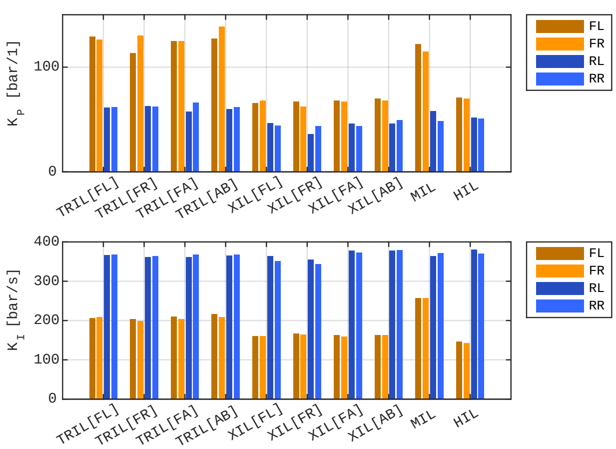

Fig. 7. Benchmark of optimization using different XIL methodologies

front axle and the parameter K_I is bigger on the rear axle. Fig. 8 shows that the ABS controller is robust. This experiment was performed on road conditions with randomized friction coefficient. The controller stabilize the vehicle and prevent wheel locks.

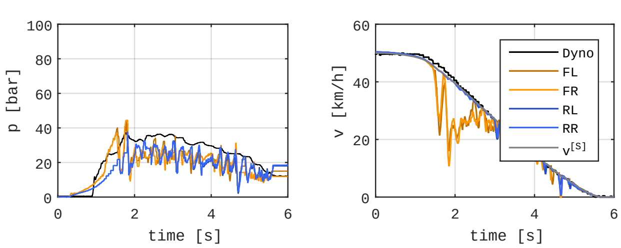

Fig. 8. Test run after SPSA optimization using XIL

V. Conclusion

Although optimization problems are often used for analysis and control, the integration of optimization methods into a XiL environment can improve outcome, confidence and robustness of the design. In conclusion the authors contributed to following topics:

(i) Optimization methods are suitable to improve or support the development process.

(ii) Stochastic methods like SPSA do not require an explicit knowledge of the system for optimization in order to create a loss function of the optimization problem. An implicit estimation of the relationship between input and output is sufficient. However, the loss function must map the optimization problem with adequate accuracy.

(iii) Since empirical data or simulation results are required to determine the gradient of the loss function, the X-in-the-Loop approach and optimization methods complete each other. However, the optimization process must be recursive or real-time capable rather.

However, further investigation is required to realize a real-time capable SPSA method for complex systems.

Acknowledgment

This project has received funding from the European Union's Horizon 2020 research and innovation programme under grant agreement No 824333.

The authors would like to thank Prof. Klaus Augsburg (former TU Ilmenau) for his support of these research activities.

References

[1] V. Schreiber, V. Ivanov, K. Augsburg, M. Noack, B. Shyrokau, C. Sandu, and P. S. Els, "Shared and distributed x-in-the-loop tests for automotive systems: Feasibility study," *IEEE Access*, vol. 6, pp. 4017–4026, 2018.

[2] V. Schreiber, K. Augsburg, V. Ivanov, and H. Fujimoto, "Novel developing environment for automated and electrified vehicles using remote and distributed x-in-the-loop technique," in *2020 IEEE Vehicle Power and Propulsion Conference (VPPC)*, 2020, pp. 1–5.

[3] P. Sadegh and J. C. Spall, "Optimal random perturbations for stochastic approximation using a simultaneous perturbation gradient approximation," in *Proceedings of the 1997 American Control Conference (Cat. No.97CH36041)*, vol. 6, June 1997, pp. 3582–3586 vol.6.

[4] J. C. Spall, "A stochastic approximation algorithm for large-dimensional systems in the kiefer-wolfowitz setting," in *Proceedings of the 27th IEEE Conference on Decision and Control*, Dec 1988, pp. 1544–1548 vol.2.

[5] J. Kiefer and J. Wolfowitz, "Stochastic estimation of the maximum of a regression function," *Ann. Math. Statist.*, vol. 23, no. 3, pp. 462–466, 09 1952. [Online]. Available: https://doi.org/10.1214/aoms/1177729392

[6] P. Sadegh and J. C. Spall, "Correction to optimal random perturbations for stochastic approximation using a simultaneous perturbation gradient approximation"," *IEEE Transactions on Automatic Control*, vol. 44, no. 1, pp. 231–232, 1999.

[7] J. C. Spall, "An overview of the simultaneous perturbation method for efficient optimization," *Johns Hopkins APL Technical Digest (Applied Physics Laboratory)*, vol. 19, pp. 482–492, 10 1998.

[8] F. Pretagostini, L. Ferranti, G. Berardo, V. Ivanov, and B. Shyrokau, "Survey on wheel slip control design strategies, evaluation and application to antilock braking systems," *IEEE Access*, vol. 8, pp. 10 951–10 970, 2020.

[9] D. Savitski, D. Schleinin, V. Ivanov, and K. Augsburg, "Robust continuous wheel slip control with reference adaptation: Application to the brake system with decoupled architecture," *IEEE Transactions on Industrial Informatics*, vol. 14, no. 9, pp. 4212–4223, Sep. 2018.